



# Structural, Optical and Dielectric Studies of $\text{Zn}_{0.975}\text{Mg}_{0.025}\text{O}$ Oxide Material

Tarun Garg, M. Saleem#

Govt. (Model, Autonomous) Holkar Science College, Indore (M.P.) India-452001.

**Abstract:**  $\text{Zn}_{0.975}\text{Mg}_{0.025}\text{O}$  oxide material synthesized by solid state reaction method. The sample has been characterized for structural studies using reliable technique known as X-ray diffraction characterization. For optical band gap estimation, the diffuse reflectance UV-Vis spectra was collected and analyzed. For electrical properties, we carried out frequency dependent dielectric measurement, The XRD data study revealed the sample has acquired hexagonal structure. Optical band gap of the sample was found to be 3.11eV. The dielectric measurement of the sample revealed the sample is a good dielectric material. Also the electrical measurement witness semiconducting nature of the sample under investigation.

**Keywords:** Transition metal oxides, structure; doping, bandgap; dielectric properties

**Corresponding author e-mail;** [msephy7@gmail.com](mailto:msephy7@gmail.com)

## Introduction

Transition metal oxides are hot spot of the advanced technological applications. Researchers have explored them from different aspects, yet a huge is expected. Their technological applications can be enhanced from the synthesis point of view, doping, bulk, nano and thin film formation etc. Although all the transitional metals are equally important, but zinc oxide has fascinated the research community due to its ubiquitous properties. Zinc oxide (ZnO) is II–VI semiconductor with a direct wide band gap (3.37 eV at 300 K). It has high optoelectronic efficiencies as compared to indirect band gap semiconductor [1]. The greatest challenge for optoelectronic applications remains the fabrication of efficient and reliable p-type. Researchers interest is fascinated recently by ZnO based compounds. In the near past, a more sophisticated phenomenon such as resistive switching, i.e., electric-field-induced oxygen vacancies migration, which is an intrinsic property of ZnMgO, has been investigated as potentially detrimental to operational stability [2-4].

The uses of ZnO as a photocatalytic degradation material has been extensively studied. Preparation of nano-size ZnO has been carried out by different methods like hydrothermal method, aerosol, micro-emulsion, ultrasonic, sol–gel method, evaporation of solution and suspensions, evaporative decomposition of solution (EDS), solid state reaction, conventional ceramic fabrication, wet chemical synthesis, spray pyrolysis

method [5-9]. However to emphasize on its different physical properties, we synthesized ZnMgO by solid state reaction.

Magnesium oxide remained interesting from long time for several important phenomena like; defect induced magnetism, spin electron reflectivity, broad laser emission etc. Moreover, nanostructures of this material exhibited suitability for different kinds of applications ranging from wastewater treatment to spintronics depending upon their shape and size. In this way, researchers had grown nanostructures in the form of nanoparticles, thin films, nanotubes, nanowalls, nanobelts. Though nanoparticles and thin films are well known form of nanostructures and wide variety of synthesis approaches are available, however, limited methodology for other nanostructures are available [10,11].

Zinc oxide has wide direct band gap, the large exciton binding energy, and a high radiation stability. By virtue of these unique properties, it is considered as a promising material for the improvement of optoelectronic devices operating in the violet and ultraviolet regimes. A key technology toward the realization of such applications is the synthesis of the ternary compounds ZnCdO, ZnMgO, etc. These compounds were found to exhibit band gap of the order of 2.99 eV and 5.3 eV. Furthermore, feasibility of ZnO based optoelectronic device is witnessed from the realization of heterostructures and quantum wells in this compound. Zinc oxide (ZnO) is used as a heterogeneous catalyst, have a high catalytic activity, non-toxic, insoluble, and also a cheap catalyst which is an important n-type semiconductor [12-15].

In the present work the influence of the Mg doping in ZnO and the variation of the physical properties has been systematically investigated. The investigated properties include structural, optical bandgap, and dielectric properties.

## Experimental Details

### Preparation

The  $Zn_{0.975}Mg_{0.025}O$  oxide material was synthesized by the solid state reaction method. The employed solid state route comprises of the following steps

### Weighing ⇒ Mixing ⇒ Calcination ⇒ Grinding ⇒ Pelletization ⇒ Sintering

In this report, the  $Zn_{0.975}Mg_{0.025}O$  oxide material was synthesized using zinc oxide (ZnO) and magnesium oxide (MgO) as starting materials. The quantities of these oxides as required by the formula were mixed in an agate-mortar via hard mechanical grinding for 6h. The mixed materials were calcined for 6h at 1000 °C. The final was re-ground for 6h and calcined at 1100 °C for 5h. The so calcined mixture was ground for 1h to obtain the final fine powder. The powder is mixed with PVA, a binder for pellet formation. Circular discs of 10mm in diameter and width of 1mm were formed at a pressure of 5tonnes per inch. The pellets so formed were sintered at 1200 °C for 5h to get hard and compact form of materials for future experimentation. The sample in powder form is also ready for the characterization.

## Experimentation

The  $\text{Zn}_{0.975}\text{Mg}_{0.025}\text{O}$  oxide material synthesized via solid state route was examined for structural, optical and dielectric properties. The phase formation was verified exploiting Bruker D8 Advanced spectrometer. UV-Vis spectrometer from Perkin Elmer, Lambda 950—USA, was employed to record the diffuse reflectance spectra for the estimation of optical bandgap. The samples were subjected to dielectric measurements exploiting the instrument of a Model E4980A Precision LCR meter (2 Hz–2 MHz) from Keysight Technologies.

## Results and Discussions

### XRD analysis

The  $\text{Zn}_{0.975}\text{Mg}_{0.025}\text{O}$  oxide material synthesized by solid state reaction method were investigated for structural and phase formation exploiting XRD technique. We collected diffraction data in the angular range of  $20^\circ - 80^\circ$ . The data was plotted and displayed as **Figure 1**. The cleanliness and absence of noise and extra diffraction peaks reveals the sample is single phased in nature. The analysis of the pattern infer that the sample has acquired hexagonal wurtzite structure and the assigned space group is  $P6_3mc$  [16]. The sharpness of the diffraction and hence their higher intensity witness the sample inherits higher crystallinity.

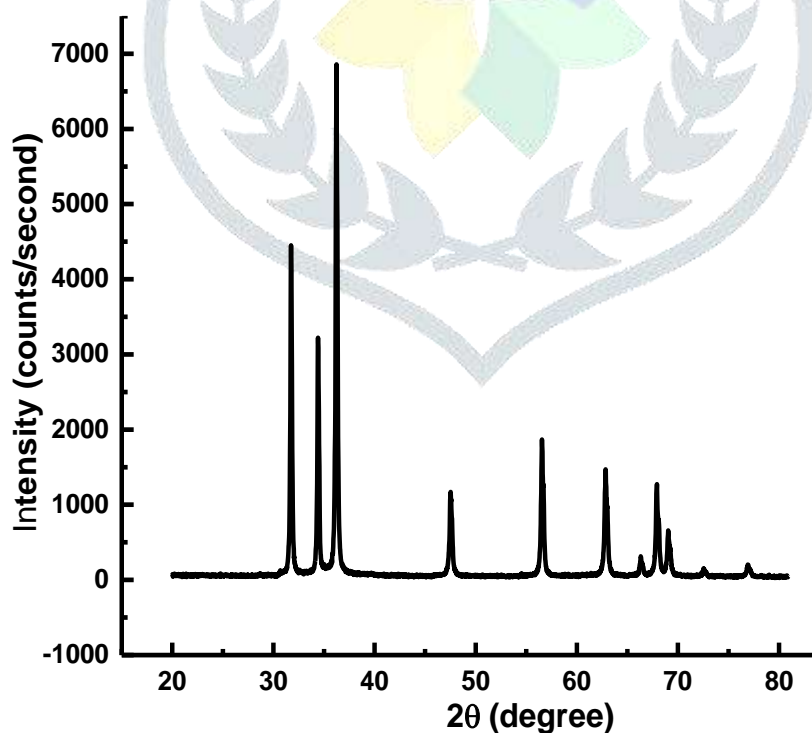


**Figure 1: XRD pattern of  $\text{Zn}_{0.975}\text{Mg}_{0.025}\text{O}$  oxide material**

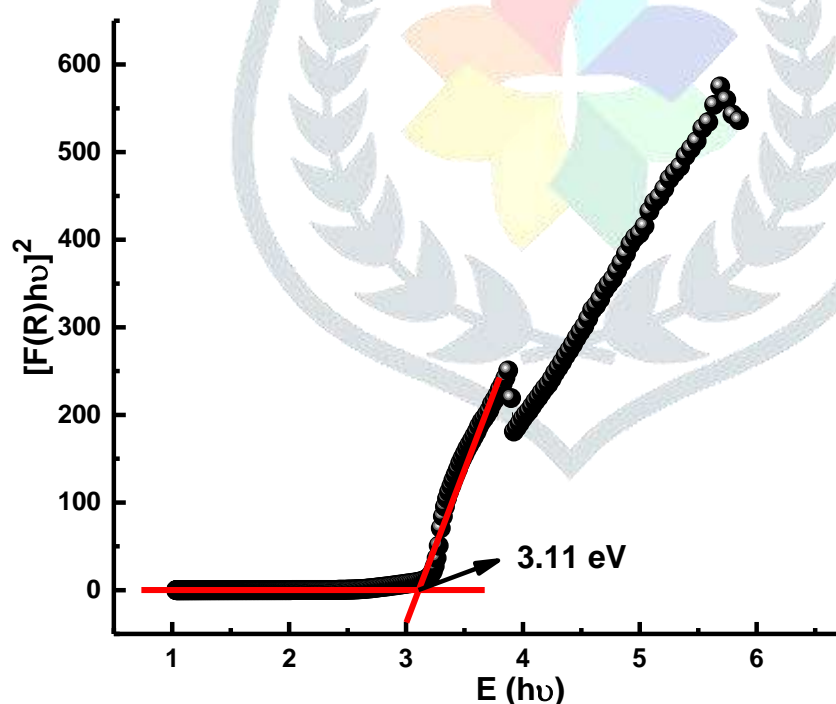
The moderate width i.e. moderate full width at half maximum (FWHM) of the characteristic peaks of the XRD pattern of  $\text{Zn}_{0.975}\text{Mg}_{0.025}\text{O}$  oxide material is indicative that the sample exhibits comparatively small average crystallite size. The crystallite sizes of the sample have been calculated using classical Scherer's

formula,  $t = k\lambda / [\beta \cos\theta]$ , where  $t$  is thickness,  $\lambda$  is wavelength of X-ray used (1.5406 Å),  $k$  is a constant (shape factor  $z$  0.9),  $\theta$  is the angle of diffraction, and  $\beta$  is the FWHM, and the average size of the crystallites was 66 nm. The lattice parameters, volume and size were calculated which confirm the crystallization of the sample into the hexagonal structure. The calculated parameters were  $a = b = 3.25$  Å and  $c = 5.20$  Å and volume =  $47.56$  Å<sup>3</sup>. The diffractions were indexed according to wurtzite hexagonal structure as **Figure 1** displays.

### UV-Vis Studies for Optical Bandgap Determination

For  $Zn_{0.975}Mg_{0.025}O$  oxide material, we carried out the UV-Vis diffuse reflectance spectroscopic measurements to investigate the optical energy band gap. **Figure 2** shows the UV-Visible spectrum of  $Zn_{0.975}Mg_{0.025}O$  oxide. To determine the optical band gap energy, we used Tauc's relation in the form of Kubelka-Munk function  $F(R) = (1 - R)^n / 2R$  where  $R$  is reflectance and  $n$  is transition-dependent integer [17] against the energy ( $h\nu$ ). In the present case, we obtained the best fit by plotting  $[h\nu F(R)]^n$  against  $h\nu$  for  $n = 2$ , i.e., allowed indirect transition. The optical band gap value was obtained by extrapolating a straight line along the sharp edge of the curve that cuts the energy axis at certain point. The intercept made by extrapolated line on the energy axis is the energy band gap value [18].

**Figure 2: Tauc's Plot for  $Zn_{0.975}Mg_{0.025}O$  oxide material**



### Dielectric Properties

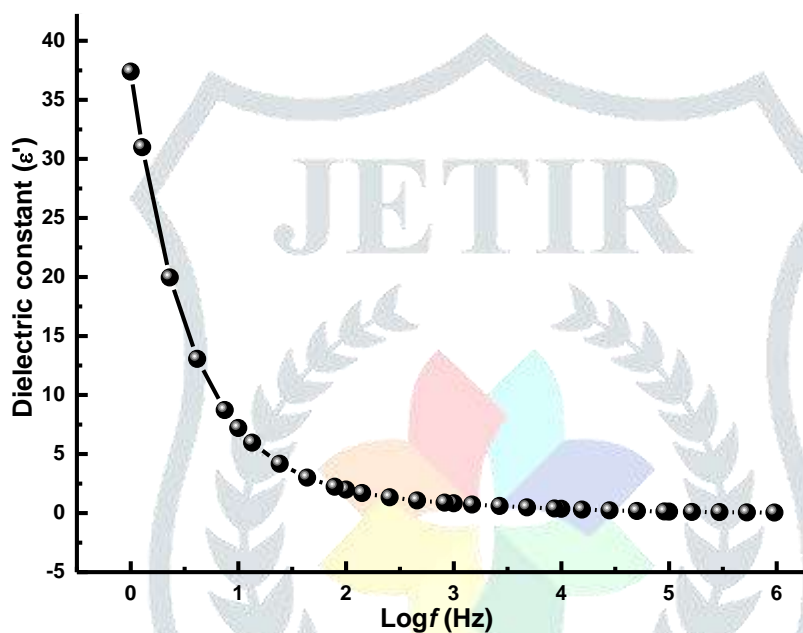
#### Dielectric Constant

The dielectric constant ( $\epsilon'$ ) studies of  $Zn_{0.975}Mg_{0.025}O$  oxide material have been carried out over frequency range of 100Hz–1 MHz and the data has been displayed as a function of frequency in **Figure 3**. The variations of dielectric constant ( $\epsilon'$ ) display the usual trend of decrease in  $\epsilon'$  with increase in frequency. It is clear from **Figure 3** that the dielectric constant declines rapidly as frequency increases, until it reaches

a constant value at higher frequency. This behavior of dielectric constant occurs as the electronic exchange between the metal ions does not obey the applied field after a certain limit of the applied field [19-22]. The large value of the dielectric constant at low frequency indicates dielectric dispersion due to space-charge polarization. As the frequency increases, the ionic and orientation polarizabilities fall and finally their contribution becomes insignificant, owing to the inertia of the molecules and ions. The dielectric constant of the sample exhibit dispersion at low frequencies, which can be explained by Koop's model and Maxwell-Wagner polarization theory [21-23].

**Figure 3: Dielectric constant of  $Zn_{0.975}Mg_{0.025}O$  oxide material**

When subjected to an electric field, these space charges move and are trapped by defects resulting in the formation of dipole moments. This implies that the regions of lower frequency have a permanent



dipoles which align themselves along the direction of the field and contribute to the total polarization of the dielectric material. On the other hand, at higher frequency, the variation in field is too rapid for the dipoles to align themselves in the direction of field, i.e., dipoles can no longer follow the field, so their contribution to the total polarization and hence to the dielectric constant becomes smaller. In MHz region, the charge carriers would barely have started to move before the field reversal occurs and  $\epsilon'$  falls to a small value at higher frequencies [22, 23].

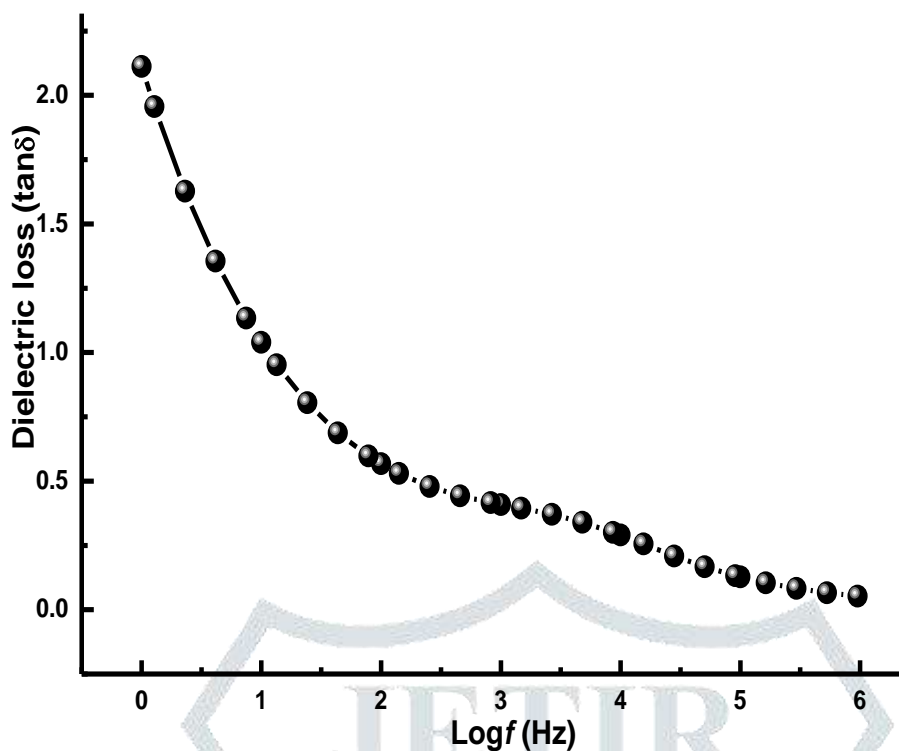


**Figure 4: Dielectric loss of  $\text{Zn}_{0.975}\text{Mg}_{0.025}\text{O}$  oxide material**

The room temperature dielectric loss ( $\tan\delta$ ) has been investigated for the prepared sample. Figure 4 displays the dielectric loss which conveys that with increase of frequency, dielectric loss ( $\tan\delta$ ) of the sample decreases. Decrease in dielectric loss observed at higher frequency are due to suppression of domain wall motion. The value of dielectric loss tangent is high at low frequency and progressively reduces and attains a lower value at higher frequency region. The dielectric loss arises if the polarization lags behind the applied alternating field which is introduced by the presence of impurities and structural inhomogeneities. The dielectric loss is maximum at lower frequencies where hopping frequency between different ionic sites and the frequency of the applied field is nearly same [24, 25].

From Figure 5, it is observed that initially the value of ac conductivity remains constant and a limit reaches after which the conductivity starts increasing abruptly with further increase in the applied field. The physics behind this character is that after a certain value of applied field i.e. threshold frequency, the trapped charge gets released and increase in the field increases the kinetic energy of the de-trapped charge carriers resulting in the abrupt increase in ac conductivity. Further, the conductivity of Mg doped ZnO is lower useful for storage applications [26,27].

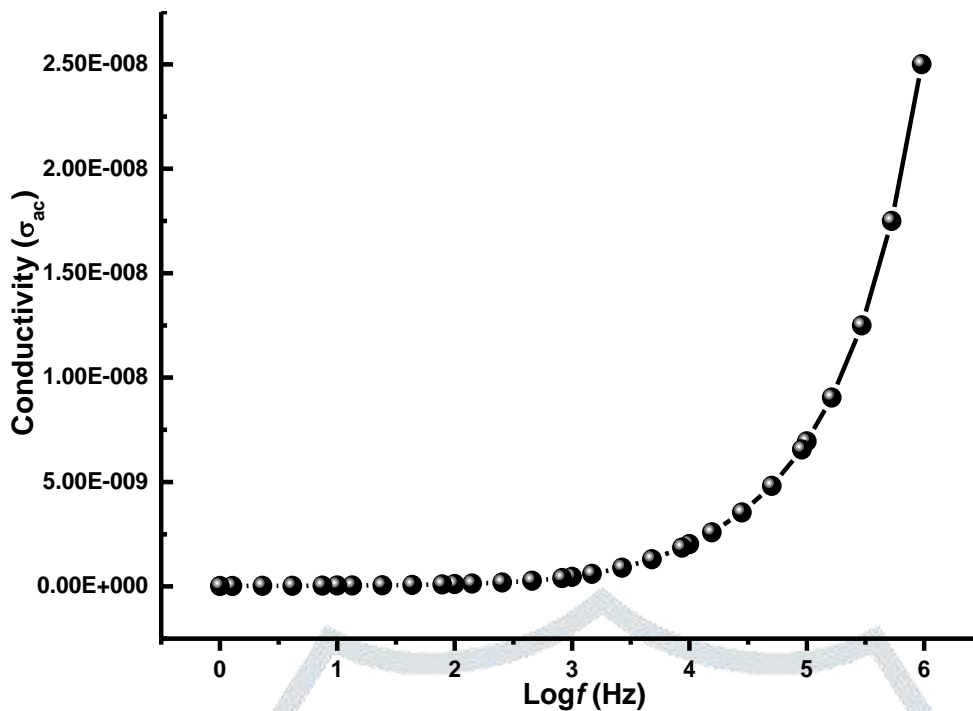


Figure 5; ac conductivity of  $Zn_{0.975}Mg_{0.025}O$  oxide material

## Conclusions

The  $Zn_{0.975}Mg_{0.025}O$  oxide material was successfully synthesized and characterized for structural, optical and dielectric properties. The XRD analysis inferred the sample has crystallized into wurtzite hexagonal structure with space group  $P_{63}mc$ . The sample has been found to be wide bandgap material feasible for electric device applications. Further, we have witnessed the sample to exhibit relatively high dielectric constant and small loss values. This feature witness its application in optoelectronic applications. The *ac* conductivity of the sample is indicative that the sample is semiconducting in nature.

## Acknowledgements

Authors acknowledge UGC-DAE CSR, as an institute for extending its facilities. Authors acknowledge fruitful guidance of Dr. M. Gupta for XRD characterization, Dr. R. Rawat for dielectric measurement and Dr. U. Deshpande for UV-Vis spectral data acquisition. Engineers related to these instruments at UGC-DAE CSR, Indore are also acknowledged.

## References

- [1] S. C. Singh and R. Gopal, *Physica E* 40, 724 (2008).
- [2] K. Karthik, S. Dhanuskodi, C. Gobinath and S. Sivaramakrishnan, *Molecular and Biomolecular Spectroscopy* 139, 7 (2015).
- [3] B. M. Weckhuysen, A. A. Verberckmoes, J. Daebaere, K. Ooms, I. Langhans and R. A. Schoonheydt, *J. Molecular Catalysis A: Chemical* 151, 115 (2000).

- [4] M. Karimi, J. Saydi, M. Mahmoodi, J. Seidi, M. Ezzati, S. S. Anari and B. Ghasemian, *J. Phys. Chemistry of Solids* 74 1392 (2013)
- [5] K G Kanade et al. *Mater Res Bull.* 41, 590 (2006).
- [6] M. Sabbaghan et al. *Solid State Sci.:* 14, 1191 (2012).
- [7] E. Darezereshki, *Appl Clay Sci.:* 54,107 (2011).
- [8] H. Wang, et al. *Powder Technol.;* 239, 266 (2013).
- [9] Suchanek WL. *J Cryst Growth.;* 312 100 (2009)
- [10] J. P. Singh, V. Singh, A. Sharma, G. Pandey, K, H, Chae, S. Lee, *Heliyon* 6, 04882 (2020)
- [11] Y. Abdallah et. al., *BioMed Res. Int.* 2019, 5620989 (2019)
- [12] M. Tortosa, M. Mollar, and B. Mari, *J. Cryst. Growth* 304, 97 (2007)
- [13] A. Ohtomo, M. Kawasaki, T. Koida, K. Masubuchi, H. Koinuma, Y. Sakurai, Y. Yoshida, T. Yasuda, and Y. Segawa, *Appl. Phys. Lett.* 72, 2466 (1998)
- [14] T. S. Jeong, M. S. Han, J. H. Kim, S. J. Bae, and C. J. Youn, *J. Phys. D* 40, 370 (2007).
- [15] T. Gruber, C. Kirchner, R. Kling, F. Reuss, and A. Waag, *Appl. Phys. Lett.* 84, 5359 (2004)
- [16] M. Saleem, A. Mishra, *Chinese Journal of Physics* 61 (2019) 166–179
- [17] J Tauc *Optical properties of solid's F Abeles (ed.) (Amsterdam: North Holland Publishers) (1970)*
- [18] M. Saleem, S. Tiwari, M. Soni, N. Bajpai and A. Mishra, *International Journal of Modern Physics B*, 34, 2050033(2020)
- [19] K.L. Nagi, J.N. Mundy, H. Jain, O. Iianert, G. Balzer Jollenkck, *Phys. Rev. B* 39 (1984) 6169.
- [20] K.W. Wagner, *Zur theorie der unvollkommenen dielektrika, Ann. Phys.* 40, 817 (1913)
- [21] C. G. Koops, *Phys. Rev.* 83, 121 (1951)
- [22] M. S. Samuel, J. Koshy, A. Chandran, K.C. George, *Physica B* 406, 3023 (2011).
- [23] N. Rezhlescu, E. Rezhlescu, *Phys. Stat. Soli. A* 23, 575 (1974)
- [24] M. Saleem, A. Mishra, D. Varshney, *Mater. Res. Express* 6, 026304 (2019)
- [25] M. Ashokkumar, S. Muthukumaran, *Powder Technol.* 268, 80 (2014)
- [26] G. Paramesh, R. Vaish, K.B.R. Varma, *J. Non Cryst. Solids.* 357, 1479 (2011).
- [27] M. Krichen, M. Megdiche, K. Guidara, M. Gargouri, , *Ionics* 21, 935 (2015)